Electronic structure and Fermi surface of strongly ferromagnetic U_2N_2Z-type (Z=Sb,Te,Bi) compounds from first principles

M. Samsel-Czekała

Institute of Low Temperature and Structure Research, Polish Academy of Sciences, P.O. Box 1410, 50-950 Wrocław 2, Poland and Leibniz-Institut für Festkörper- und Werkstoffforschung, IFW Dresden, PF 270116, D-01171 Dresden, Germany

(Received 8 April 2009; revised manuscript received 22 June 2009; published 24 July 2009)

The electronic structures of the uranium ternaries of the U_2N_2Z-type (Z=Sb,Te,Bi), crystallizing in the tetragonal $I4/mmm$ structure and having among uranium systems relatively high values of both their ferromagnetic (FM) transition temperatures and ordered magnetic moments (mms), have been investigated *ab initio*. They were calculated employing the local-spin density-functional theory with different versions of the orbital polarization correction (OPC) applied within the fully relativistic and full potential local-orbital band-structure code. The obtained results predict all these materials to be metallic both in the ferromagnetically ordered and nonmagnetically ordered (NMO) states. However, the bottoms of their conduction bands in the NMO states occur merely about 0.3 eV below the Fermi level, E_F, and a pronounced gap in U_2N_2Te or pseudogaps in the two remaining compounds are opening just below these bands, which makes such a metallic state unstable. The considerable reduction in these gap or pseudogaps in the FM states cause a stabilization of a metallic behavior. A covalently metallic bonding character of these ternaries has been obtained in all calculations. It appeared that the only uranium atoms create predominantly metallic bonding due to a fairly strong hybridization between the U 5f and U 6d electrons. The U 5f electrons contributing also to the covalent bonding have somewhat dual character, i.e., partly localized and itinerant. Contrary to the Sb- and Bi-based ternaries ordered along the c axis, as deduced from previous neutron powder diffraction studies, U_2N_2Te has a canted FM structure with its mms tilted from the c axis by about 70°. This fact has also been revealed by the present theoretical results. These data also point to the fact that the telluride, unlike the two other compounds, exhibits an almost half-metallic behavior. For all three ternaries, using the OPXC version of OPC the computed mms are in accord with the published experimental data. In turn, the Fermi surfaces of investigated ternaries have quasi-two-dimensional properties and quite unique nesting features along directions of their easy magnetization axes.

DOI: 10.1103/PhysRevB.80.045121 PACS number(s): 71.27.+a, 71.20.−b, 71.18.+y, 75.30.Gw

I. INTRODUCTION

Magnetic studies performed on a series of the U_2N_2Z-type (Z=Sb,Te,Bi) compounds, reported many years ago by Troć and Żołnierek[1,2] demonstrated interesting and worth further studies magnetic properties. All these compounds crystallize in the same tetragonal structure of the U_2N_2Sb-type (space group: $I4/mmm$, no. 139).[3] The latter structure visualized in Fig. 1 as SbN_2U_2 becomes isostructural to the very common one of $ThCr_2Si_2$ type. In addition, these ternaries containing the Sb and Bi atoms are isoelectronic since they have the same kind and number of valence electrons: $5s^25p^3$ and $6s^26p^3$, respectively, whereas the Te atom has one 5p electron more ($5s^25p^4$) than Sb. The magnetic measurements showed that all the considered here ternaries are ferromagnetic (FM) with relatively high (among uranium systems) Curie temperatures T_C (=166, 154, and 71 K for Sb, Bi, and Te, respectively).[1,2] For all of them, the neutron powder diffraction studies[4] confirmed that the uranium atoms are ferromagnetically ordered but indicated some different magnetic structures depending on the number of valence electrons. It appears that for the Sb- and Bi-based ternaries the magnetic moments (mms) are arranged along the elongated c axis, while for U_2N_2Te the mms are tilted from this axis by about 70°.[5] Experimental values of the total ordered, μ_{tot}, (effective) mms in μ_B units are as follows: 2.50 (2.65) for U_2N_2Te; 1.80 (1.78) for U_2N_2Sb, and 1.95 (1.85) for U_2N_2Bi.[1,2,4,5] It is worth noticing that the ordered and effective moments in this group of compounds are almost equal to each other due to the specific ground state (for explanation see Ref. 2).

For a better demonstration of the above experimental results in the form that has been not published yet, Fig. 2 presents the dependence of T_C vs μ_{tot} for the three compounds that is monotonically decreasing. Among the systems studied, U_2N_2Te has the highest values of both types of mms although it exhibits the lowest T_C. The upper inset to this figure illustrates values of μ_{tot} depending on the shortest U-U distance, $d_{U\text{-}U}$, in each compound, while the lower inset plots the T_C vs $d_{U\text{-}U}$ curve, which interestingly decreases linearly. In the tetragonal U_2N_2Z-type compounds, two different type $d_{U\text{-}U}$ occur depending on Z. For Z=Te, this is the distance between atoms within the same U layer, perpendicular to the c axis, while for Z=Sb and Bi, $d_{U\text{-}U}$ separates atoms lying in neighboring parallel U layers. It turns out that $d_{U\text{-}U}$ for Z=Te is much larger than those for the two other ternaries (see Table I and Fig. 2). All the three $d_{U\text{-}U}$ values are well above so-called Hill limit of 0.34 nm, which is a critical value for the onset of magnetism in actinide systems.[6] As expected for a simple scenario when one has to do mainly with an U 5f-6d hybridization, the larger $d_{U\text{-}U}$ the higher values of μ_{tot}, which is well followed by these compounds (see upper inset to Fig. 2). However, it is curious why with increasing $d_{U\text{-}U}$ distances and simultaneously μ_{tot} values, the Curie temperatures exhibit so strong decreasing tendencies (plotted in Fig. 2) as in the case of, e.g., FM uranium monochalcogenides.[7]

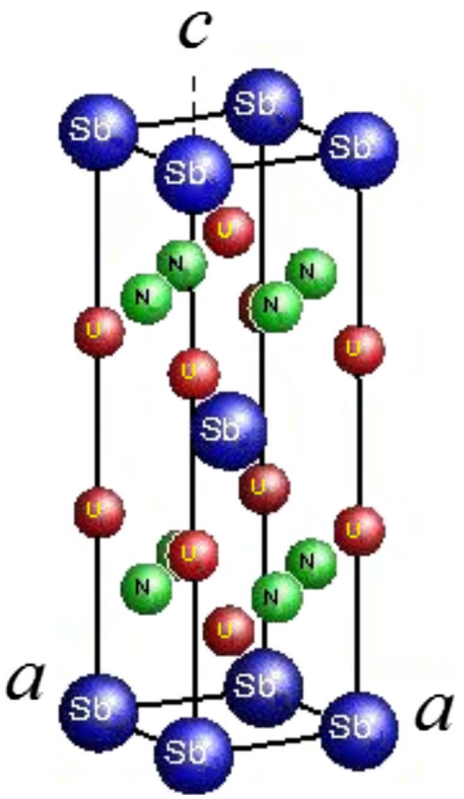

FIG. 1. (Color online) The crystal structure $I4/mmm$ of the U_2N_2Sb-type.

Furthermore, this type of compounds containing uranium and nitrogen (e.g., see a number of papers on UN)[8] arises a great interest in chemical bondings, because of a large difference in the atomic sizes, having also an influence on magnetism. Therefore, a prediction of their band structures seems to be important for future experiments. Very recent papers considering chemical aspects of the U-N bondings have

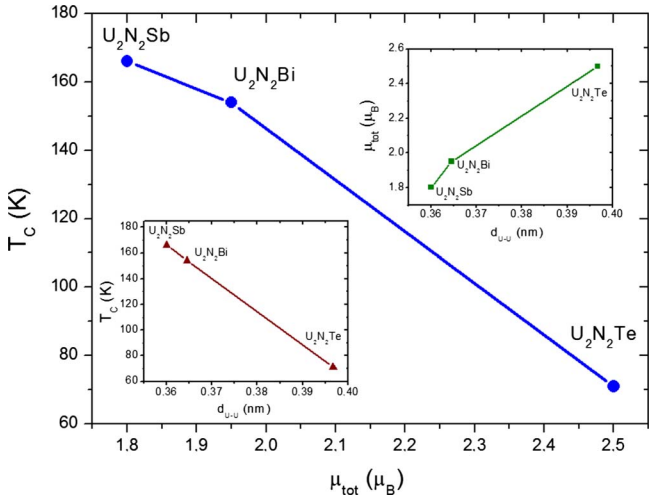

FIG. 2. (Color online) The dependence of T_C vs ordered μ_{tot} for U_2N_2Z-type compounds based on the results reported in Refs. 1, 2, 4, and 5. The upper inset shows the dependence of μ_{tot} on the shortest U-U distance, d_{U-U}, and the lower inset plots the T_C vs d_{U-U} curve in these compounds.

TABLE I. Experimental values of the lattice parameters a and c (in nm) and free parameter z, used in the calculations, as well as the shortest distances between uranium atoms, d_{U-U}.

Compound	a	c	z	d_{U-U}
U_2N_2Sb	0.38937[a]	1.23371[a]	0.344[a]	0.360
U_2N_2Te	0.3967[b]	1.258[b]	0.3399[c]	0.3967
U_2N_2Bi	0.39292[a]	1.2548[a]	0.344[a]	0.365

[a]Reference 3.
[b]Reference 2.
[c]Reference 5.

demonstrated that they are covalentlike and only uranium atoms create metalliclike bonding.[9,10] Unfortunately, no results of band-structure calculations for the U_2N_2Z-type compounds have been published up to now.

To investigate chemical bonding and an origin of strong magnetism occurring in these U_2N_2Z-type systems, in the present paper their electronic and magnetic structures have been calculated based on the density-functional theory (DFT).[11] The fully relativistic and full-potential local-orbital (FPLO) minimum basis code[12] was applied within the local (spin) density approximation [L(S)DA]. Moreover, having at disposal experimental values of the total FM-ordered moments in these three compounds, determined directly from the neutron-diffraction measurements,[2,4,5] this group of systems is an ideal candidate to investigate efficiency of different versions of the orbital polarization correction (OPC) (Ref. 13) that can be suitable to describe large values of the total ordered mms in these compounds. The experimental lattice parameters and atomic positions, previously obtained in the powder x-ray and neutron diffraction experiments of these ternaries,[2,3,5] were taken to compute band energies, $E_n(\mathbf{k})$, densities of states (DOSs), Fermi surfaces (FSs), occupation numbers (N), and magnitudes of the ordered mms. In order to evaluate the magnetocrystalline anisotropy energies (MAE), the values of the total energy of a given compound were determined assuming the different crystallographic orientations of its ordered mms.

II. COMPUTATIONAL DETAILS

The band structures of the U_2N_2Z-type ternaries have been computed by the fully relativistic versions of the FPLO method.[12] In this modern method the four-component Kohn-Sham-Dirac equation, containing implicitly spin-orbit coupling (SOC) up to all orders, is solved self-consistently. The Perdew-Wang parametrization[14] of the exchange-correlation potential is used in LSDA with and without different versions of OPC such as OPB, OPXC, and OPX (Ref. 13) applied to the U $5f$ electrons. The OPB correction is a modification of *so-called* Brooks' OPC (analogous to the spin polarization) in which the term $-1/2\Sigma \boldsymbol{l}_i \cdot \boldsymbol{l}_j$ ($\boldsymbol{l}_i$ is an angular momentum for ith electron in the f^n configuration) occurring in the energy of the ground state of an atom as a function of occupation number is replaced with $-1/2(\Sigma i l_i^z)(\Sigma j l_j^z)$ and, as a consequence, a term $\Delta E_l = -1/2E^3L^2$ is obtained where L is the total angular momentum and E^3 is constant so-called Ra-

cah parameter. In turn, the OPXC correction to the total energy contains only orbital polarization energy connected with correlation contribution $\Delta E_{OP}^{XC}=E_{OP}^{C,L}$, while the OPX correction to the total energy consists of only the Hartree-Fock contribution and double counting correction of full-potential LSDA, i.e., $\Delta E_{OP}^{X}=E_{OP}^{HF}-E_{OP}^{LSDA}$.

In the calculations the x-ray experimental values of the lattice parameters taken from Refs. 2 and 3 and experimental values of the free parameter z (Refs. 3 and 5) are given in Table I. In addition, the shortest distances between uranium atoms, $d_{U\text{-}U}$, are collected in this table. The unit cell (u.c.) of each studied system contains one formula unit (f.u.) and the following nonequivalent atomic positions U: $(0,0,z)$; N: (1/2,0,1/4); and Z: (0,0,0). The adopted valence basis sets were as follows: in the compounds with Bi and Sb the U states: $5p5d5f$; $6s6p6d$; $7s7p$ while in U_2N_2Te the U $5p5d$ electrons were treated as core states; the Sb and Te states: $4d$; $5s5p$ and the Bi: $5d$; $6s6p$, and N: $2s2p$; $3d$ states. The size of the k-point mesh in the Brillouin zone (BZ) of $12\times12\times12$ turned out to be sufficient.

For both the nonmagnetically ordered (NMO) and FM states, the total energy values, band energies, $E_n(\mathbf{k})$, occupation numbers, total and partial DOSs for each atomic site and for different electron orbitals, as well as values of the ordered mms have been calculated within the LDA and spin- and orbital polarized LSDA and LSDA (+OPB, OPXC, OPX) approaches. Finally, to evaluate the magnitude of MAE the values of the total energy of a given compound were computed for the following orientations of mms: [100], [001], [111], [101], and [110] in the tetragonal u.c.

III. RESULTS AND DISCUSSION

The calculated band energies, $E_n(\mathbf{k})$, of the U_2N_2Z-type systems in both the NMO and FM states within the LDA and LSDA or LSDA+OPXC approach for the mms collinear with the c axis (U_2N_2Sb) or tilted from this axis by 70° (for U_2N_2Te) are displayed in Figs. 3 and 4. Since the character of all bands in the isoelectronic U_2N_2Sb and U_2N_2Bi systems has been found to be almost identical (in the scale of these figures) in both NMO and FM states, only the case of U_2N_2Sb is displayed. A visual presentation of the results with applying OPC is limited to that for its OPXC version yielding the best agreement of the calculated values of the ordered mms with the experimental ones, which will be shown later on (see Table III).

It is apparent from Figs. 3 and 4 that the energy bands, being predominantly of a $5f$-electron character in all the three compounds, are crossing the Fermi levels, E_F, both in their NMO and FM states and, hence, the systems are basically metallic. However, in the NMO phases of all the three considered ternaries the bottoms of the conduction bands are situated merely about 0.30 eV (for U_2N_2Te) and 0.25 eV (for the two other compounds) below E_F (see also DOSs in Figs. 5 and 6). As is clearly seen in Fig. 3, U_2N_2Te has quite a large energy gap (being as wide as at least 1 eV) opening below the conduction bands. In the case of two remaining compounds there are only pronounced pseudogaps in this energy region. Hence, such a metallic state as described above can be unstable being highly sensitive to even small changes in values of the crystal lattice parameters, deviation from stoichiometry or contamination by impurities. Such changes may drive the considered here compounds, but particularly U_2N_2Te, toward a semiconducting behavior. Thus, contrary to metallic UN, one cannot preclude that in reality all of these ternaries are semiconductors. Furthermore, as demonstrated in Fig. 4 (see also Figs. 7 and 8) in the FM states of U_2N_2Te the bottoms of the conduction bands are shifted to about −0.5 and −1 eV in the cases of using the LSDA and LSDA+OPXC functionals, respectively. This is connected with a large reduction in the associated gap below E_F that transforms to a pseudogap in the case of the LSDA +OPXC data. The results based on the same approaches for the two remaining compounds, yield the magnitudes of the pseudogaps below E_F being somewhat minimized due to shifts of the bottoms of the conduction bands down to about −0.4 and −0.75 eV, respectively. As a consequence, the metallic behavior of all considered here systems in the FM states should be more stable.

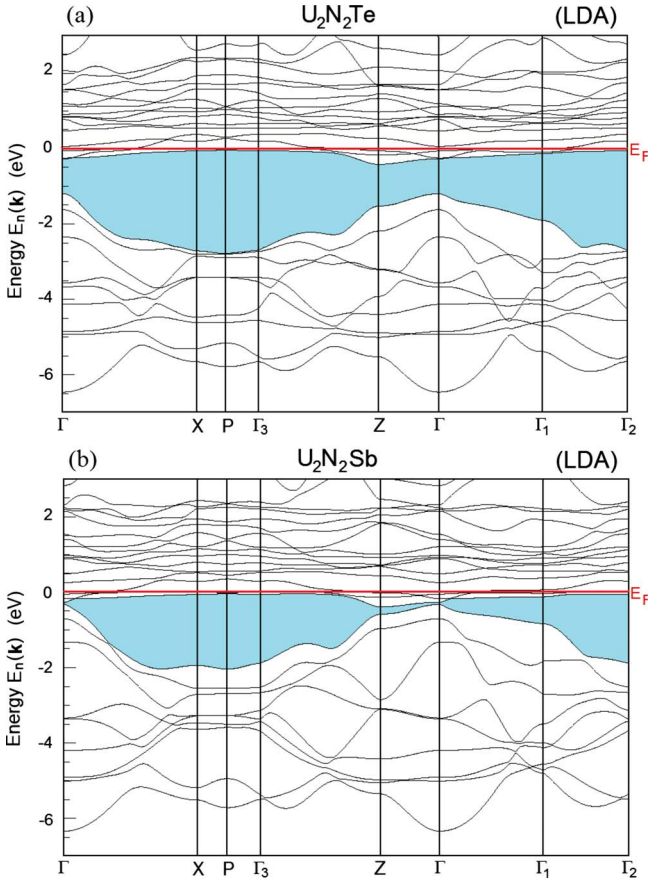

FIG. 3. (Color online) Computed band energies, $E_n(\mathbf{k})$, in the NMO state (LDA) for: (a) U_2N_2Te and (b) U_2N_2Sb compounds. The pronounced gap in the panel (a) and pseudogap in the panel (b) opening at the vicinity of E_F are marked by gray (blue) area.

The total and partial DOSs of the U_2N_2Z-type ternaries are presented in Figs. 5–8. In Fig. 5 the results of the NMO calculations are displayed in the whole energy region of valence bands ranging down to 19 eV below E_F. The positions and contributions of these dispersive bands remain practi-

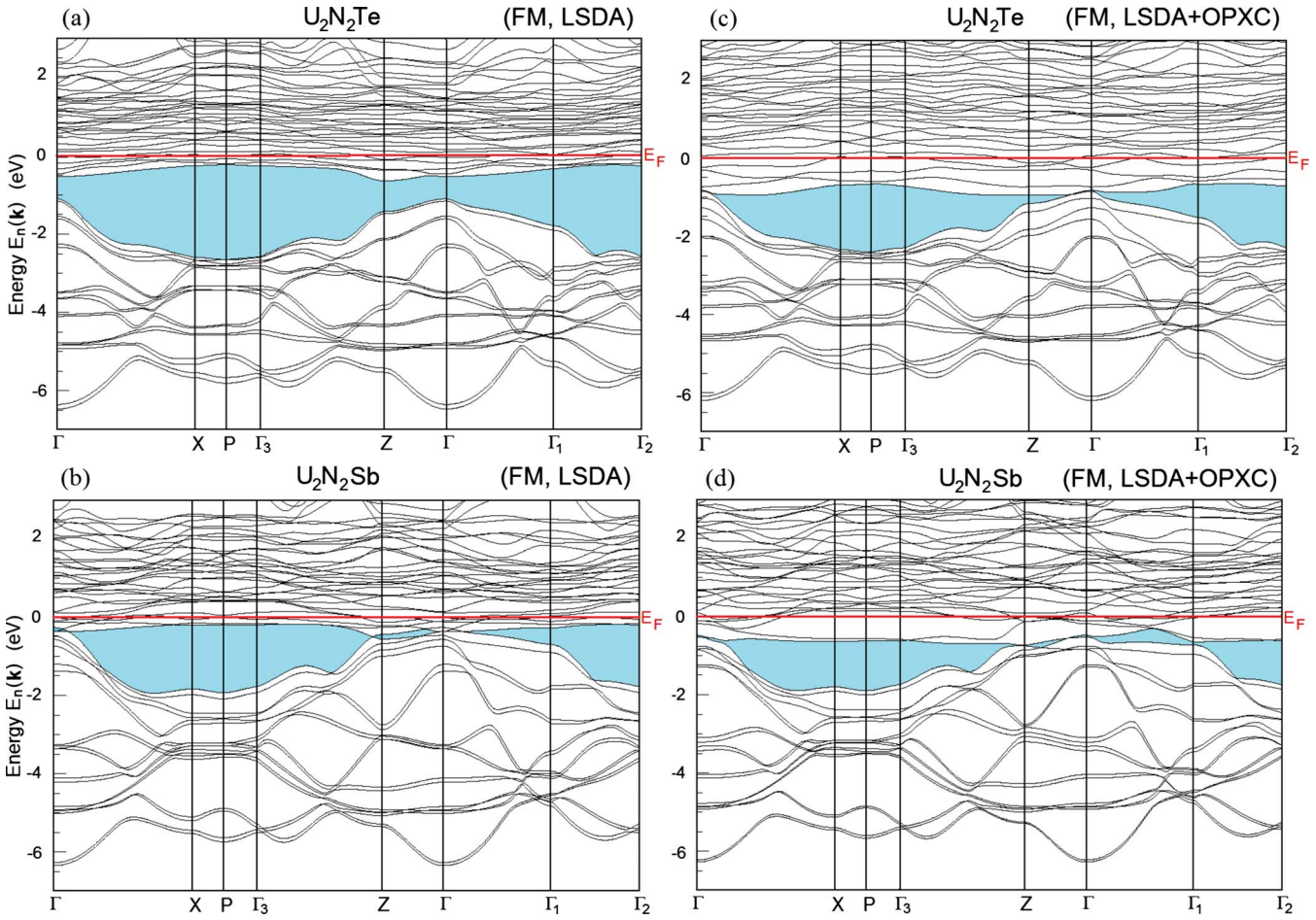

FIG. 4. (Color online) Bands as in Fig. 2 but in the FM states calculated within the: (a,b) LSDA and (c,d) LSDA+OPXC approaches for: (a,c) U_2N_2Te and (b,d) U_2N_2Sb.

cally unchanged (at least below −1.5 eV) compared to that in the corresponding FM states. In all these three compounds, the deepest valence bands located in the range of 16.5–19 eV below E_F are dominated by the contributions of the U 6*p* electrons slightly hybridized with the N 2*s* electrons and by this creating a covalent bonding between the U and N atoms. The succeeding bands occurring in energy ranges from 14.5 to 11.2 and 14.5 to 11.7 eV below E_F in U_2N_2Te and the $U_2N_2(Sb,Bi)$ ternaries, respectively, originate mainly from the U 6*p* orbitals being strongly hybridized with the N 2*s* ones. In the case of the telluride, these states are additionally mixed with the Te 5*s* electrons and they together form a covalent bonding between all kinds of constituent atoms, while in the U_2N_2Sb and U_2N_2Bi systems their Sb 5*s* and Bi 6*s* electrons create bands in the energy regions of 8.7–9.8 and 10.2–11 eV below E_F, respectively. The bottoms of the succeeding valence bands occur at 6 and 5.8 eV below E_F for the U_2N_2Te and (Sb, Bi)-based systems, respectively. It is well seen in Fig. 5 that these valence bands originate from the U 6*d* electrons being quite strongly hybridized with the U 5*f* electrons and they together with the N 2*p* and Te 5*p* or Sb 5*p* (Bi 6*p*) electrons create a covalentlike bonding between all three kinds of constituent atoms in a given system. These valence bands in U_2N_2Te within the LDA and LSDA approach (see Figs. 5–7) are more separated from the conduction bands by the energy gap of at least 1 eV wide. In comparison, in the two other systems as already mentioned, solely pseudogaps exist which only slightly separate these valence bands from the conduction ones.

Interestingly, as indicated in Figs. 5–8, the conduction bands at E_F consist of both the U 5*f* and, in a small degree, the U 6*d* electrons. It causes that the only uranium atoms form predominantly metallic bonding due to the above electrons. Moreover, these states together with the U 6*p*, N 2*sp*, and *Z* (5–6)*sp* electrons create covalent bonding between the U, N, and *Z* atoms. Such a mixed character of bonding has been obtained in calculations for all three compounds in both their NMO and FM states. This scenario is analogous to that observed for UN (Refs. 9 and 10) where also the U atoms themselves (due to their 5*f* and 6*d* electron hybridization) form metallic bonding, while there is covalent bonding between the U and N atoms.

The NMO (LDA) results for the $U_2N_2(Sb,Bi)$ systems are analogous to one another. So only the case of the antimonide is illustrated in Fig. 6. Furthermore, for all three considered ternaries the Fermi level cuts the highest top of the U 5*f* peaks in DOSs and, hence, the NMO state becomes unstable. Moreover, for U_2N_2Te in the energy range of 0.4–0.48 eV above E_F, an additional gap is opening due to SOC, while in the two remaining compounds there are again pseudogaps at about 0.53 eV above E_F.

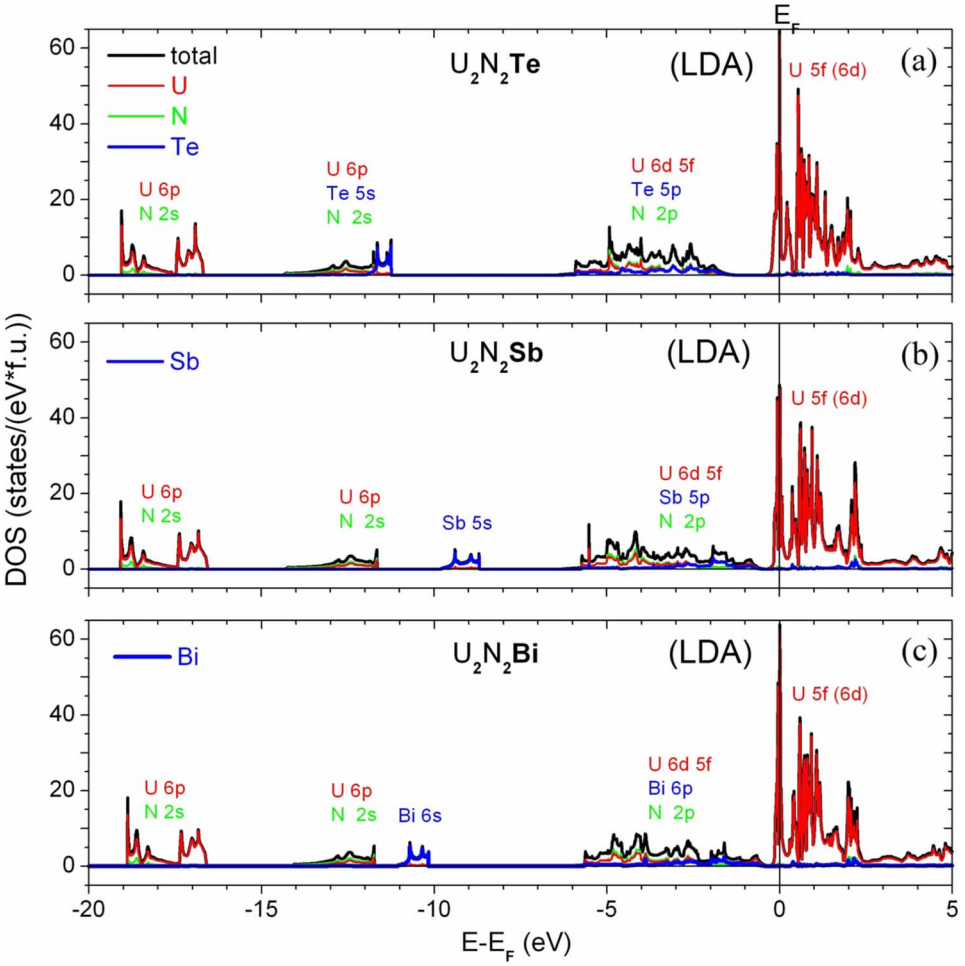

FIG. 5. (Color online) Calculated total and partial (per given atom and orbital) DOSs in the NMO (LDA) states for: (a) U_2N_2Te, (b) U_2N_2Sb, and (c) U_2N_2Bi.

In Fig. 7 where the DOSs of FM states obtained owing to the LSDA approach are plotted, it is clearly visible that in the considered systems, apart from the spreading their conduction bands down E_F, the majority (up) spins of the U 5*f* and 6*d* electrons are dominating in the energy region up to E_F and there are quite small intensity peaks of DOSs at E_F. For

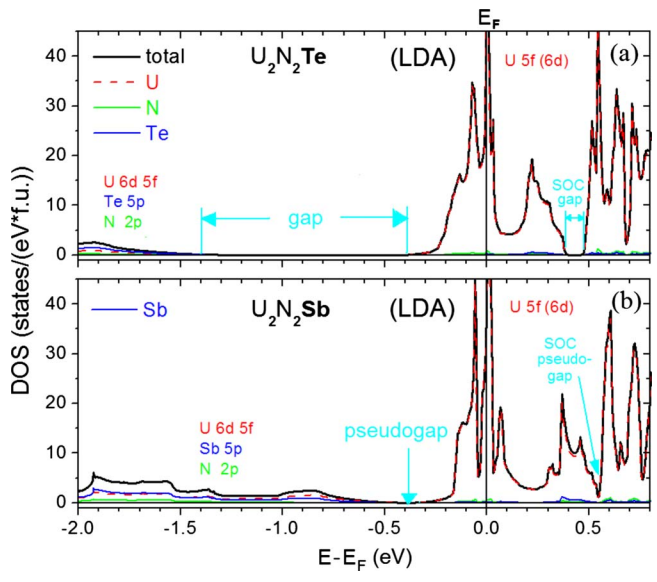

FIG. 6. (Color online) The same as in Fig. 5 but in the expanded energy scale and without the case of U_2N_2Bi which is very similar (in this scale) to that of U_2N_2Sb.

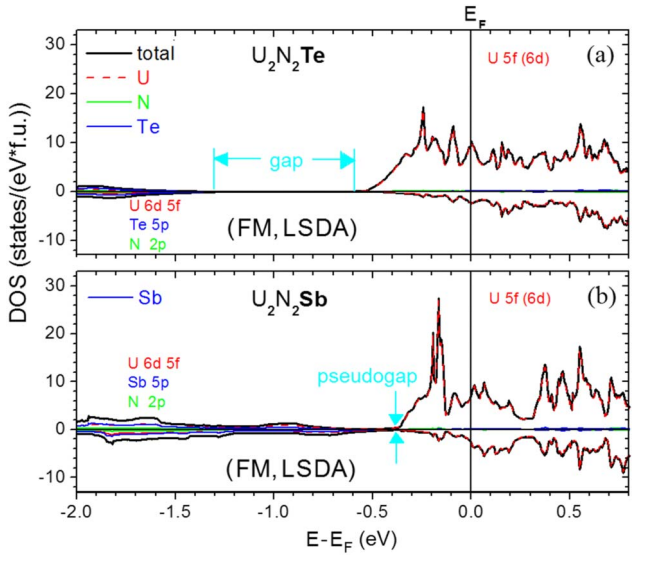

FIG. 7. (Color online) Calculated total and partial DOSs in the FM (LSDA) states for: (a) U_2N_2Te and (b) U_2N_2Sb, where spin-up and -down channels are shown separately. The case of U_2N_2Bi, being similar to that of U_2N_2Sb, is not shown here.

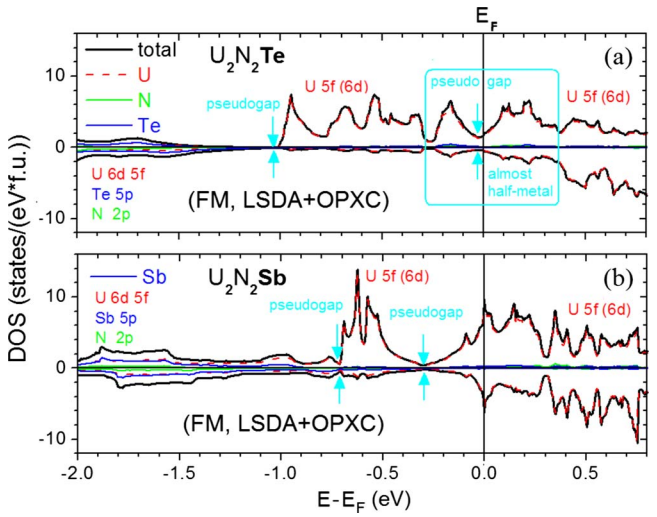

FIG. 8. (Color online) The same as in Fig. 7 but here the FM states are obtained employing the LSDA+OPXC approach.

the U_2N_2(Sb,Bi) systems (shown only for the antimonide), the highest narrow DOS peaks coming from the U 5*f* spin-up electrons are centered at about 0.17 eV below E_F. This fact can be an evidence of forming some localization state originating from the U 5*f* electrons. It is the most likely connected with their dual behavior, i.e., partly localized and partly itinerant. It should be mentioned that U_2N_2Te also calculated in the collinear FM (LSDA) state (not shown here) has some narrow peak composed of the U 5*f* spin-up electrons but laying deeper in energy, i.e., about 0.25 eV below E_F. Interestingly, this peak has as high intensity as that in the two other compounds, while for the ground state of U_2N_2Te with canted FM structure, as presented in Fig. 7(a), the analogous peak as described above has a much smaller intensity.

The most interesting results are those attributed to the FM states in the U_2N_2Z-type compounds obtained by an application of the LSDA+OPXC approach, which are displayed in Fig. 8.

As seen in the figure, the bottoms of the conduction bands in the U_2N_2Te system are shifted down to −1 eV and the gap below them is transforming to a pseudogap. Again the majority spins of the U 5*f* and 6*d* electrons in the conduction bands are dominating in the energy region up to E_F, but just at E_F itself, there are pseudogaps both in spin-up and -down channels.

As Fig. 8(a) indicates, the electron spin-down contribution in U_2N_2Te is close to zero and, hence, this compound has almost a *half-metallic* behavior. Contrastingly, this is not the case for the two other compounds (both having very similar densities in the scale of Fig. 8) that exhibit nearly equal intensities of spin-up and -down peaks of DOSs at E_F though the spin-up channels are also dominating below E_F as in the telluride. Interestingly, in all three compounds studied pronounced pseudogaps open in the region of the conduction bands at about 0.28 eV below E_F separating peaks of DOSs coming from the U 5*f* spin-up of strongly localized electrons from the contributions of more itinerant U 5*f* electrons. The peak below E_F in U_2N_2Te has a lower intensity by a factor of two compared to the other systems considered here.

TABLE II. The calculated electron occupation numbers per atom in the U_2N_2Z-type compounds (Z=Sb,Te,Bi), N_{calc} compared to that for the free atoms, N_{at}, with accuracy to 0.1.

Electron orbitals	N_{at}	N_{calc}
U 5*f*	3	3.0
U 6*d*	1	2.0
U 7*s*	2	0.4
U 7*p*	0	0.2
N 2*s*	2	1.6
N 2*p*	3	3.6
Te 5*s* (or Bi 6*s*)	2	1.9
Sb 5*s*	2	1.8
Sb 5*p* (or Bi 6*p*)	3	3.5
Te 5*p*	4	4.5

The electron populations in the U_2N_2Z-type systems (Z=Sb,Te,Bi) calculated in NMO state, N_{calc}, compared to the corresponding numbers for free atoms, N_{at}, are both given in Table II. As seen from the table, the occupation numbers of electrons in U and N atoms are the same in all three studied compounds. This table indicates that $N_{calc}=N_{at}=3$ for the U 5*f* states, which points out that they rather weakly hybridize with other states. In turn, the occupation number for the U 6*d* states is doubled with respect to N_{at}. For the U 7*s* states N_{calc} is considerably reduced compared to N_{at} while the U 7*p* states occur with small values. Also for N, Te, Sb, and Bi

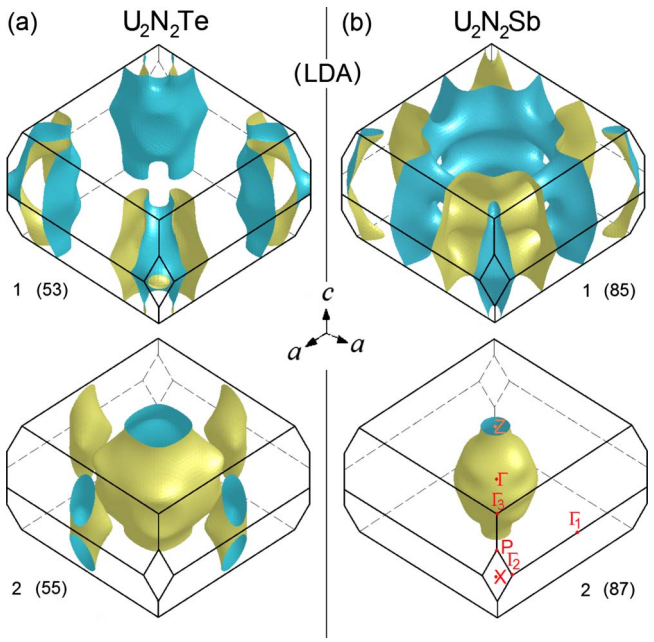

FIG. 9. (Color online) Calculated FS sheets for: (a) U_2N_2Te and (b) U_2N_2Sb in their NMO (LDA) states, existing in two Kramers double degenerated bands (see their numbers below the sheets), drawn separately in the tetragonal BZ boundaries with marked (in red color) high-symmetry points in the BZ. The dark (blue) and light (yellow) colors visualize the inside (electrons) and outside (holes) of FS, respectively.

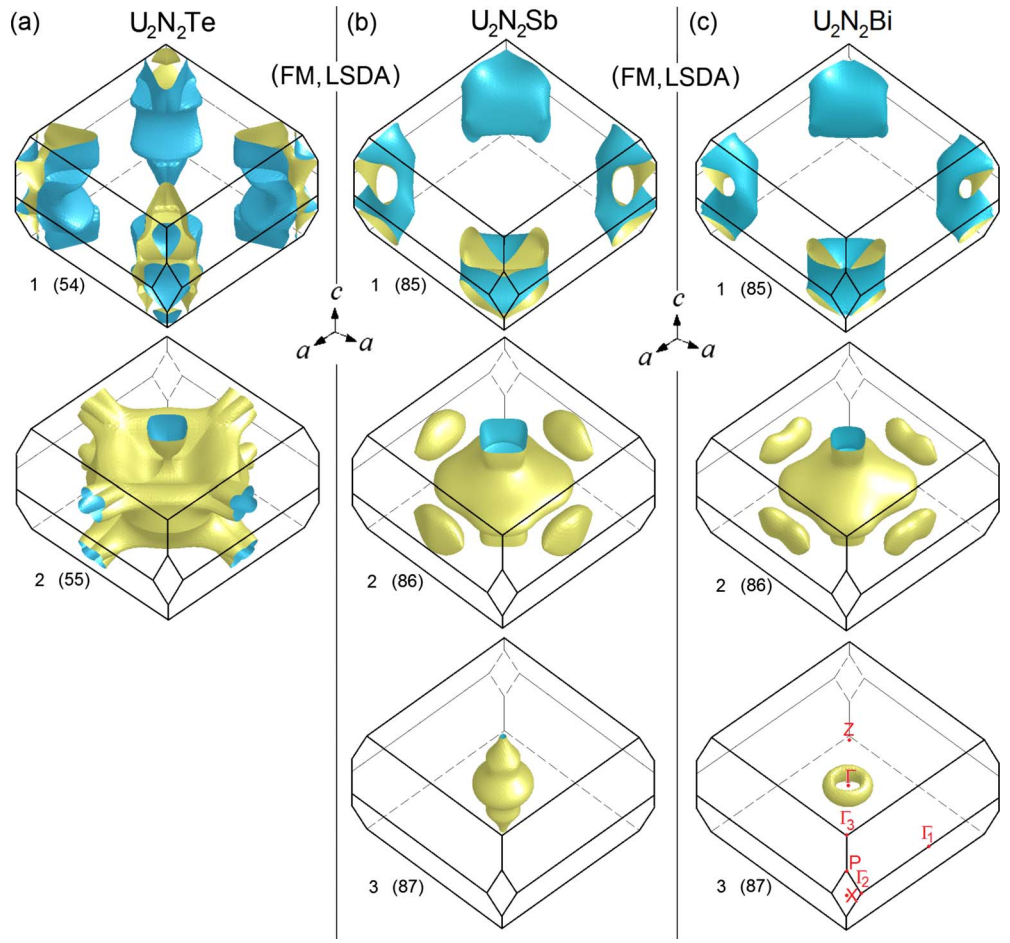

FIG. 10. (Color online) Calculated FS sheets for: (a) U_2N_2Te, (b) U_2N_2Sb, and (c) U_2N_2Bi in their FM (LSDA) ground states. The FS sheets exist in: (a) two and (b,c) three nondegenerated bands, drawn in the same convention as that in Fig. 9.

atoms their *s* electrons have lower and *p* electrons—larger N_{calc} than N_{at}. This leads to a large charge transfer of 2.6 electrons from uranium atoms to the N (1.8) and Z (0.75) ligands per f.u. All kinds of spin and orbital polarized calculations in these compounds yield almost identical results to those collected in Table II, except an unexpected LSDA +OPXC result for the U 5*f* electrons in U_2N_2Te having $N_{calc}=3.2$.

The Fermi surfaces of the NMO states of the U_2N_2Te and U_2N_2Sb systems are displayed in Fig. 9.

The FS of the U_2N_2Bi compound being identical (in the scale of the figure) with that of the isoelectronic U_2N_2Sb compound is omitted here. As presented in Fig. 9, the LDA FS sheets for each of the investigated compounds exist in two Kramers double degenerated bands, denoted in the figure by their numbers: (53,55) and (85,87) for U_2N_2Te and the two other systems, respectively. In all three compounds, there are holelike and electronlike typically metallic large FS sheets in the first and second bands, respectively, the former having quasi-two-dimensional character along the *c* axis. Since only the uranium electrons contribute to FSs, one expects somewhat weaker interaction between the U atoms along this axis.

The FS sheets of U_2N_2Te in the FM state obtained in the LSDA approach, displayed in Fig. 10(a), exist also in two but nondegenerated bands (54, 55). Both the holelike and electronlike sheets in the first and second bands are somewhat modified compared to that in its NMO state.

The FS sheets of the isoelectronic $U_2N_2(Sb,Bi)$ in their FM LSDA states, presented in Figs. 10(b) and 10(c), respectively, originate from three nondegenerated bands, numbered: (85, 86, and 87) for each compound. The holelike and electronlike FS sheets existing in the first and second bands, respectively, are very similar in both compounds, differing mainly in their sizes, while the small electronlike FS sheets in the third bands for a given compound have quite different topologies.

The most interesting cases are FSs of all three systems determined employing the LSDA+OPXC approach, visualized in Fig. 11. For each compound, there is the same number of FS sheets originating from the same bands as in the corresponding LSDA case. However, in U_2N_2Te these sheets are much reduced in their sizes being almost semimetallic-like. As seen in Fig. 12(a), the FS sheet in the first of conduction bands has distinct nesting properties[15] along the direction of the easy magnetization axis, i.e., here tilted from the *c* axis by 70°, with possible nesting vector marked in this figure. In the $U_2N_2(Sb,Bi)$ systems, the sheets in the first conduction bands are nearly identical to each other and both show almost a two-dimensional character with nesting fea-

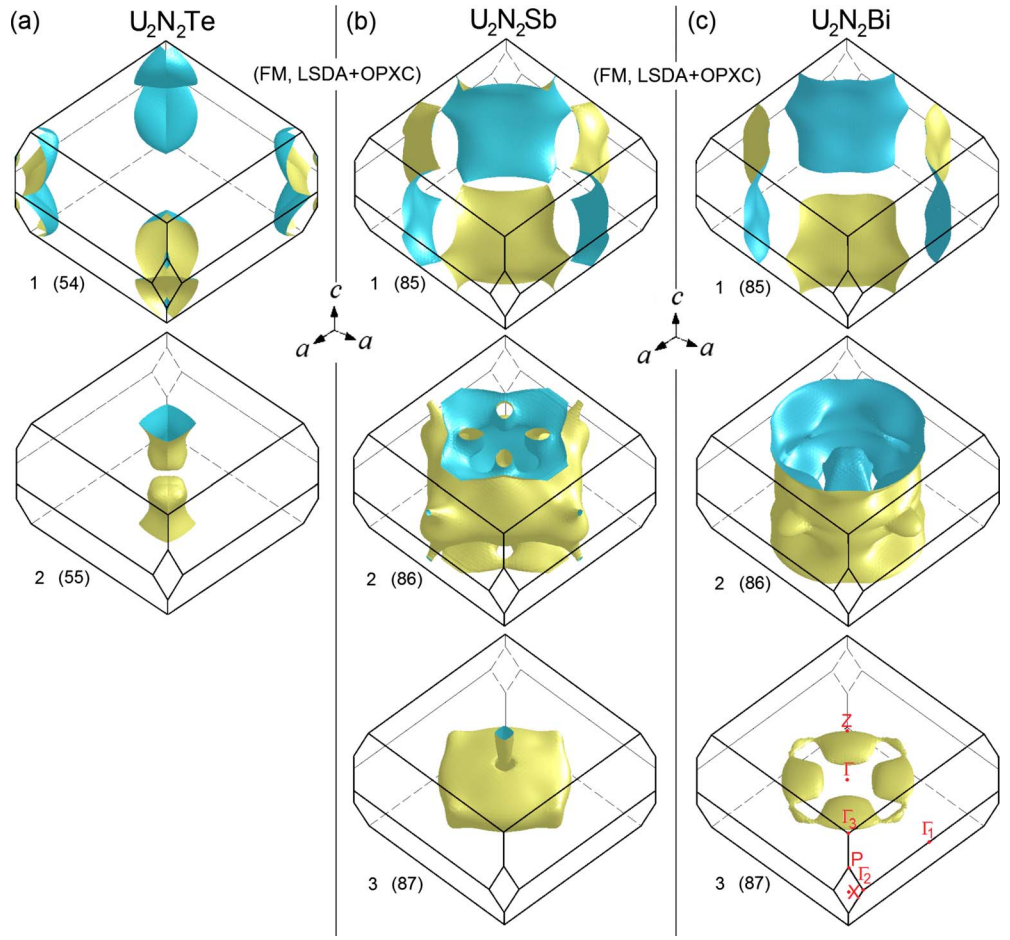

FIG. 11. (Color online) Same as in Fig. 10 but for the FM states based on the LSDA+OPXC approach.

tures along the [110] direction [see Fig. 12(c)]. This quasi-two-dimensionality of FS with nesting feature gives a possibility of arising some additional charge and/or spin density waves (CDW/SDW) as well as other exotic phenomena under some special conditions (e.g., pressure). Moreover, in all the compounds studied here the FS sheets in the second or third conduction bands have nesting properties along the easy magnetization c axis, which is clearly seen in Figs. 12(b), 12(d), and 12(e).

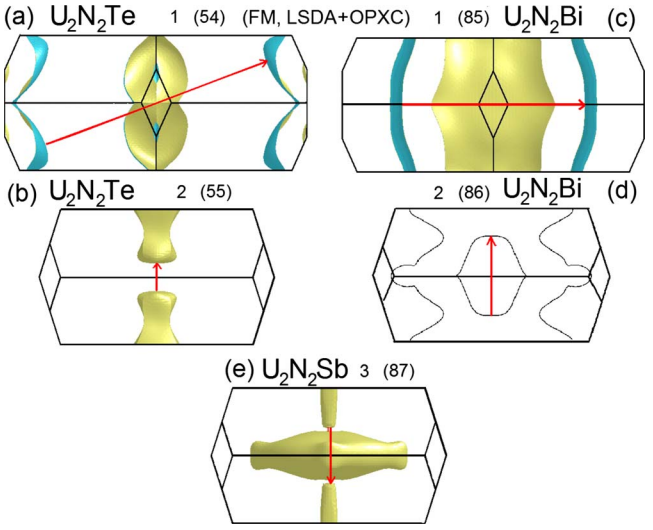

FIG. 12. (Color online) Same as in Fig. 11 but for chosen FS sheets with marked (in red) possible nesting vectors.

In all three compounds in the FM states with the magnetic moments arranged along the c axis have always lower energy than that in the NMO states by about 5 and 30 mHartree for the LSDA and LSDA+OPXC approaches, respectively. For U_2N_2Sb and U_2N_2Bi the c axis is confirmed to be an easy magnetization axis, however, the MAE between the c axis ([001]) and the other main directions: [100], [110], [101], and [111] within the LSDA approach is rather small not exceeding 0.5 mHartree. It is worth noticing that the LSDA calculations also indicate that for U_2N_2Te the canted FM structure has lower energy (by about 0.5 mHartree) than that collinear one as well as that along the above mentioned main directions, which is in agreement with neutron experiments. The LSDA MAE between the tilted direction and the others is, however, small except for the case of the [101] and [110] directions for which it ranges about 20 mHartree and for this directions the NMO state has even lower energy. For U_2N_2Te the LSDA+OPXC results also show that the canted structure is more energetically preferable (by 12 mHartree) than that with the collinear arrangement along the c axis but for the [100] direction the total energy appears to be slightly lower (by about 1 mHartree).

TABLE III. Values of spin (μ_s), orbital (μ_l), and total (μ_{tot}) FM mms aligned along the *c* axis, for U_2N_2(Sb,Bi), and tilted from this axis by 70° for U_2N_2Te, obtained by employing various approximations of exchange-correlation functionals.

		FM-ordered moments per one uranium atom (in μ_B)			
Compound	Functionals	μ_s	μ_l	μ_{tot}	experimental $\lvert\mu_{tot}\rvert$[a–d]
	LSDA	1.75	−2.15	−0.40	
	LSDA+OPXC	1.75	−4.66	**−2.91**	
	LSDA+OPX	1.78	−3.87	−2.09	
U_2N_2Te	LSDA+OPB	1.78	−3.53	−1.75	2.50
	LSDA	1.29	−1.55	−0.26	
	LSDA+OPXC	1.23	−3.38	**−2.15**	
	LSDA+OPX	1.35	−2.58	−1.23	
U_2N_2Sb	LSDA+OPB	1.34	−2.40	−1.06	1.80
	LSDA	1.35	−1.62	−0.27	
	LSDA+OPXC	1.24	−3.51	**−2.27**	
	LSDA+OPX	1.40	−2.64	−1.24	
U_2N_2Bi	LSDA+OPB	1.39	−2.46	−1.07	1.95

[a]Reference 1.
[b]Reference 2.
[c]Reference 4.
[d]Reference 5.

The values of uranium mms calculated for directions along the easy magnetization axes using various approximations of the exchange-correlation potential are collected in Table III and, for better illustration, they are plotted in Fig. 13. It is apparent from these table and figure that the LSDA approach gives decidedly too small values of the total mms $|\mu_{tot}|$ (lower than $0.5\mu_B$) compared the experimental values (of around $2\mu_B$). It turns out that the LSDA+OPXC functional yields the best agreement of $|\mu_{tot}|$ with the experimental values for all the three investigated compounds. The theoretical OPXC (and experimental) values of $|\mu_{tot}|$ in μ_B are as follows: 2.91 (2.50) for U_2N_2Te; 2.15 (1.80) for U_2N_2Sb, and 2.27 (1.95) for U_2N_2Bi.[1,2,4,5] It should be emphasized that the LSDA+OPXC approach is completely *ab initio* since it does not require any external fitting parameters, as e.g., U and J in the commonly used LSDA+U *nonab initio* approaches, and it can be employed as an alternative to the LSDA+U method in evaluation of expected large values (around $2\mu_B$ and more) of the ordered mms in other uranium compounds.

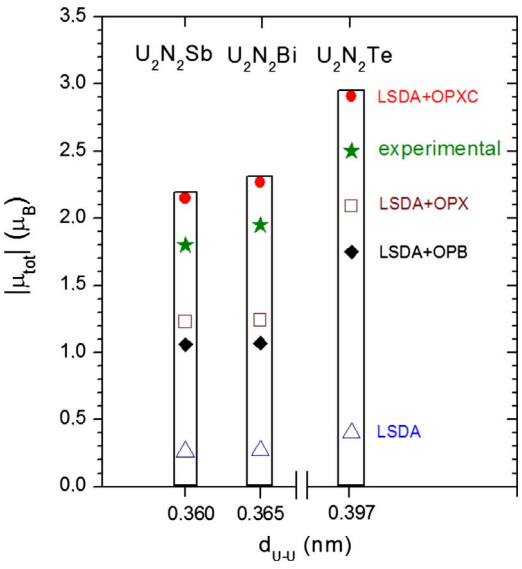

FIG. 13. (Color online) Values of total (μ_{tot}) FM mms taken from Table III for the U_2N_2Z-type compounds, calculated by employing various approximations of exchange-correlation functionals and experimental ones. On the bottom of the diagram, only values of the shortest U-U distances, $d_{U\text{-}U}$, are given while real proportions between them are drawn on a realistic scale in the insets to Fig. 2.

IV. CONCLUSIONS

Electronic and magnetic structures of the U_2N_2Z-type (Z = Sb, Te, Bi) systems adopting the same tetragonal $I4/mmm$ crystal structure have been calculated employing the FPLO code. A mixed character of atomic bonding having a covalently metallic character in all of the investigated compounds has been predicted by the computations. Only the U 5*f* and 6*d* electrons create a metallic bonding in these ternaries but in some part they also contribute to covalentlike bonding. The U 5*f* electrons seem to posses a dual character (simultaneously partly localized and partly itinerant) in all the three systems studied. U_2N_2Te exhibiting a canted FM structure, confirmed by the calculations, has almost half-metallic properties. However, one of the most interesting feature for all considered here ternaries is their band structure with gaps or pseudogaps close to E_F in the NMO states, which are considerably reduced in their FM states causing that a metallic state becomes more stable. Also the fact that

the U 5*f* sharp peaks occur at or near E_F is worth underlining here. Successfully, the OPXC version of the *ab initio* orbital polarization correction yields a fairly good agreement in mms values of the FM states with the reported experimental results and can be recommended for other uranium compounds with relatively large values of the ordered magnetic moments on U atoms. Moreover, the Fermi surfaces of these ternaries exhibit distinct nesting properties along their easy magnetization axes and quasi-two-dimensional features along the *c* axis. Finally, in all these three compounds described here the evaluated magnitudes of the differential magnetocrystalline anisotropy energies are rather small. On the basis of the presented results, one expects in the future interesting bulk physical measurements for these ternaries performed on the suitable bulk or single-crystalline samples, prepared owing to a modern technological preparation especially under pressure.

ACKNOWLEDGMENTS

I am very grateful to R. Troć for his critical reading of this paper and also thankful for technical assistance by U. Nitzsche at IFW-Dresden computers.

[1] R. Troć and Z. Żołnierek, *Proceedings International Conference On Magnetism* (Nauka, Moscow, 1975), Vol.6, p. 59.
[2] Z. Żołnierek and R. Troć, J. Magn. Magn. Mater. **8**, 210 (1978).
[3] R. Benz and W. H. Zachariasen, Acta Crystallogr. B **26**, 823 (1970).
[4] Z. Żołnierek, Ph.D. thesis, INTiBS PAN, Wrocław, 1976 (unpublished).
[5] J. Leciejewicz, Z. Żołnierek, and R. Troć, Solid State Commun. **22**, 697 (1977).
[6] H. H. Hill, in *Plutonium and Other Actinides*, edited by W. N. Miner (American Institute for Metallurgical Engineers, New York, 1970), p. 2.
[7] R. Troć, *Pnictides and Chalcogenides III (Actinide monochalcogenides)*, edited by H. P. J. Wijn, Landolt-Börnstein, New Series, Group III, Vol. 27B6β (Springer-Verlag, Berlin, 2006), p. 103.
[8] R. Troć, *Pnictides and chalcogenides III (Actinide monopnictides)*, edited by H. P. J. Wijn, Landolt-Börnstein, New Series, Group III, Vol. 27B6α (Springer-Verlag, Berlin, 2006), p. 74.
[9] M. Samsel-Czekała, E. Talik, P. de V. Du Plessis, R. Troć, H. Misiorek, and C. Sułkowski, Phys. Rev. B **76**, 144426 (2007).
[10] R. Atta-Fynn and A. K. Ray, Phys. Rev. B **76**, 115101 (2007).
[11] P. Hohenberg and W. Kohn, Phys. Rev. **136**, B864 (1964); W. Kohn and L. J. Sham, *ibid.* **140**, A1133 (1965).
[12] FPLO-5.00-18 and 5.10-20 [improved version of the original FPLO code by K. Koepernik and H. Eschrig, Phys. Rev. B **59**, 1743 (1999)] (http://www.FPLO.de).
[13] OPC implementation in FPLO5.10–20 according to O. Eriksson, M. S. S. Brooks, and B. Johansson, Phys. Rev. B **41**, 7311 (1990) [OPB]; H. Eschrig, M. Sargolzaei, K. Koepernik, and M. Richter, Europhys. Lett. **72**, 611 (2005) [OPXC, OPX]; Carsten Neise, Ph.D. thesis Technische Universität, Dresden, 2007 (http://www.ifw-dresden.de/institutes/itf/diploma-and-phd-theses-at-the-itf).
[14] J. P. Perdew and Y. Wang, Phys. Rev. B **45**, 13244 (1992).
[15] S. B. Dugdale, H. M. Fretwell, M. A. Alam, G. Kontrym-Sznajd, R. N. West, and S. Badrzadeh, Phys. Rev. Lett. **79**, 941 (1997); M. Biasini, G. Kontrym-Sznajd, M. A. Monge, M. Gemmi, A. Czopnik, and A. Jura, *ibid.* **86**, 4616 (2001); D. Hughes, M. Däne, A. Ernst, W. Hergert, M. Lüders, J. Poulter, J. B. Staunton, A. Svane, Z. Szotek, and W. M. Temmerman, Nature (London) **446**, 650 (2007).